

Chapter - 6

Proton and Magnesium Ion Conducting Polymer Electrolytes Based Solid State Batteries

Proton and Magnesium Ion Conducting Polymer Electrolytes Based Solid State Batteries

This chapter is devoted to the studies on fabrication and characterization of all-solid-state batteries based on optimised proton and magnesium ion conducting polymer/gel polymer electrolytes. The preparation and optimisation of polymer/gel electrolytes have been described in Chapters 3, 4 and 5. As mentioned earlier, the electrical conductivity of proton conducting polymer electrolytes (nanocomposites) possess the conductivity of the order of $\sim 10^{-4} \text{ S cm}^{-1}$ at room temperature. The magnesium ion conducting composite gel polymer electrolytes and ionic liquid based gel polymer electrolytes offer conductivity of the order of $\sim 10^{-3}$ - $10^{-2} \text{ S cm}^{-1}$ at room temperature. These materials are in the form of free-standing films with good mechanical strength, flexible enough to mould in desirable area and thickness. The order of conductivity is acceptable for their use in battery applications as they offer low resistance when used in the form of films of the thickness ~ 100 - $400 \mu\text{m}$. Being the flexible materials, these are able to form proper interfacial contacts with anode and cathode materials.

The proton and magnesium batteries under the present studies are described below in detail.

6.1 Proton Conducting Nanocomposite Polymer Electrolytes based Batteries

In order to fabricate proton batteries, the nanocomposite polymer electrolyte has been optimized in terms of their desirable properties for battery applications such as the electrical conductivity, thermal, mechanical and electrochemical stability. The nanocomposite polymer electrolytes selected for this purpose are PEO: NH_4HSO_4 (92:8 w/w) +3 wt.% SiO_2 (solution cast) and PEO: NH_4HSO_4 (80:20 w/w) +15 wt.% SiO_2 (hot-pressed). These compositions are selected on the basis of detailed studies, presented in Chapter 3. Suitable negative and positive electrode materials (anode and cathodes) have been prepared to fabricate proton batteries. These proton batteries have been studied by discharging them through different load resistances. Various parameters have been evaluated such as discharge capacity, specific power and specific energy etc. The details are described in the following sections.

6.1.1 Preparation of Electrode Materials

The $\text{Zn}+\text{ZnSO}_4 \cdot 7\text{H}_2\text{O}$ composite has been used as anode. It was prepared by mixing zinc dust with $\text{ZnSO}_4 \cdot 7\text{H}_2\text{O}$ in the 3:2 weight ratio, then pressed to form a pellet of thickness $\sim 1\text{mm}$. The cathode materials were prepared in the film form (thickness ~ 300 - $400 \mu\text{m}$) by hot-pressing the homogeneous mixtures of MnO_2 + graphite (C) (3:2 ratio) + polymer electrolyte and layered oxides PbO_2 + V_2O_5 +C (7:2:1 ratio) + polymer electrolyte. Graphite

(C) was added to introduce the electronic conductivity while the addition of electrolyte helped in reducing the electrode polarization. The total cell dimensions were of thickness ~ 2-3 mm and area ~1.2 cm².

6.1.2 Fabrication and Characterization of Solid State Proton Batteries

The proton batteries of the following configurations were fabricated by sandwiching nanocomposite polymer electrolyte films between anode and cathode pellets:

Cell #1: Zn + ZnSO₄.7H₂O | PEO : NH₄HSO₄ (92:8 w/w) +3 wt.%SiO₂ | MnO₂ + C

Cell #2: Zn + ZnSO₄.7H₂O | PEO : NH₄HSO₄ (92:8 w/w) +3 wt.%SiO₂ | PbO₂ + V₂O₅ + C

Cell #3: Zn+ZnSO₄.7H₂O | PEO : NH₄HSO₄ (80:20 w/w) +15 wt.%SiO₂ | MnO₂+ C
(Hot-pressed)

Cell #4: Zn+ZnSO₄.7H₂O | PEO : NH₄HSO₄ (80:20 w/w) +15 wt.%SiO₂ | PbO₂+V₂O₅+ C
(Hot-pressed)

These cells were put in desiccator for their characterization. The open circuit voltage (OCV) and cell potential measurements were carried out with the help of a high impedance digital multimeter (ESCORTS 97). The batteries were discharged under different load conditions (1 MΩ and 100 KΩ) and the cell potentials were monitored as a function of time.

To check the initial voltage obtainable from the fabricated cell and to ensure proper electrode-electrolyte contacts, open circuit voltage has been measured over a period of ~ 24 h, as shown in Fig. 6.1. Open circuit voltage values 1.8 V, 1.5 V, 1.7 and 1.5 V were obtained for Cells #1, #2, #3 and #4, respectively. It can be seen that after very small initial

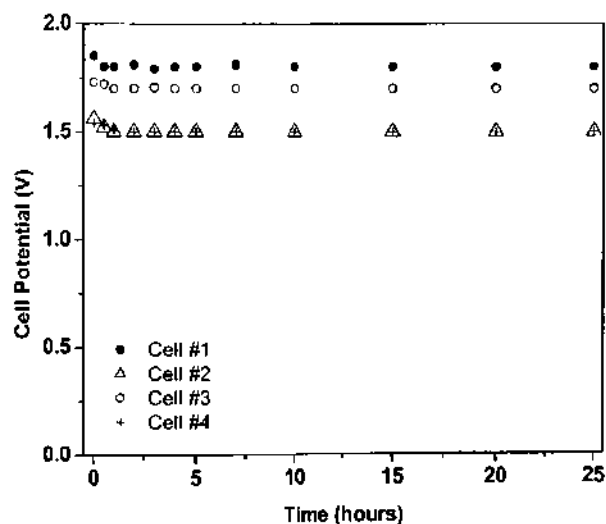


Fig. 6.1: Variation of open circuit voltage (OCV) of different cells with time.

drop the voltage remained constant for a period of 24 h. This shows that fabricated cells have been stable in open circuit condition.

All the batteries were discharged through $1\text{ M}\Omega$ and $100\text{ K}\Omega$ loads at room temperature. Fig. 6.2 (a & b) and Fig. 6.3 (a & b) show the cell-potential variation as a function of time for the two load resistances, respectively. One can note that all the batteries performed fairly well when they have been discharged through a high load resistance (i.e. $1\text{ M}\Omega$) or during the low current drain. A small initial drop in the cell potentials have been observed, which is due to the usual cell polarization effect. However, the battery discharged relatively quickly with $100\text{ K}\Omega$ load. Table 6.1 lists some important battery parameters evaluated in the plateau region of $1\text{ M}\Omega$ discharge profile of Cells #1-4.

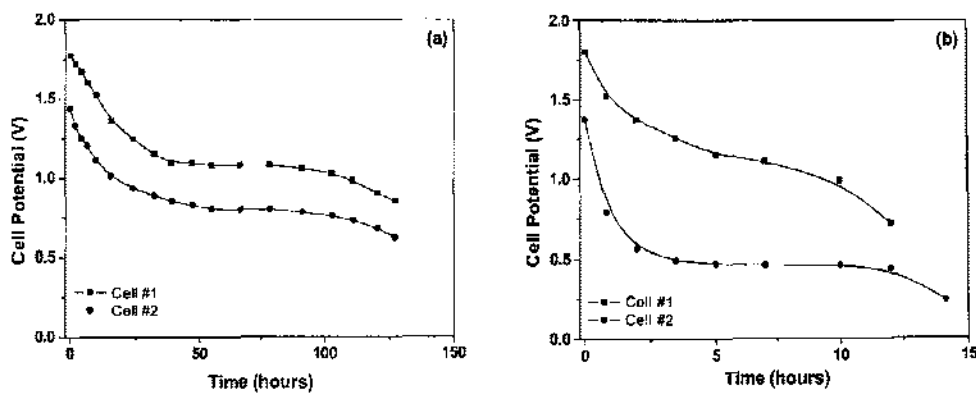


Fig. 6.2: (a) Cell voltage as a function of time for cells #1 and #2 at $1\text{ M}\Omega$; (b) Cell voltage as a function of time for cells #1 and #2 at $100\text{ K}\Omega$.

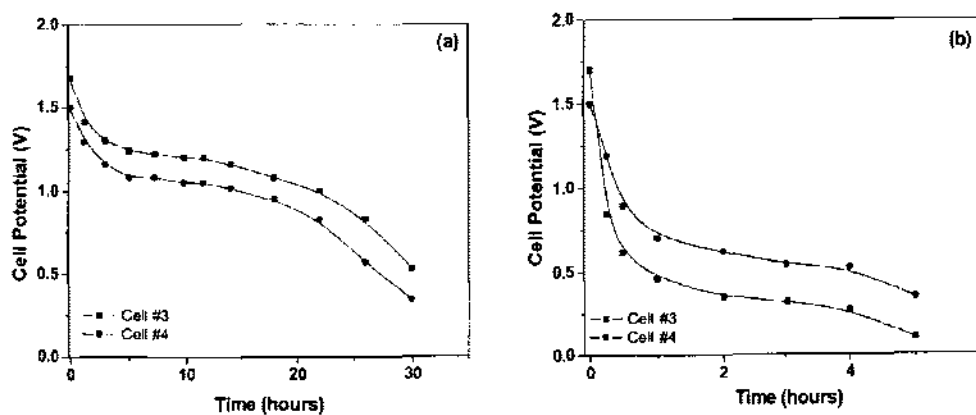


Fig. 6.3: (a) Cell voltage as a function of time for cells #3 and #4 at $1\text{ M}\Omega$; (b) Cell voltage as a function of time for cells #3 and #4 at $100\text{ K}\Omega$.

Table 6.1: Some Important Parameters of proton batteries (Cells # 1-4).

Parameters	Cell #1	Cell #2	Cell #3	Cell #4
Cell weight (mg)	600	600	500	500
Cell area (cm ²)	1.2	1.2	1.2	1.2
Open-circuit voltage (V)	1.8	1.5	1.7	1.5
Current density (μAcm^{-2})	218	85	26	22
Discharge capacity (μAh)	2.3	1.4	3.4	2.4
Specific energy (mWhkg^{-1})	1.0	0.75	1.1	0.92
Specific power (mWkg^{-1})	110	122	68	48

6.2 Mg²⁺ Ion Conducting Gel Polymer Electrolytes Based Rechargeable Batteries

As elaborated in section 1.4.1 of Chapter 1, the performance capabilities of magnesium-based rechargeable battery systems are expected to be close to the lithium-based rechargeable batteries. The present section reports the fabrication of all solid state magnesium batteries and the studies on charge-discharge performance of the magnesium cells based on the newly synthesized Mg²⁺ ion conducting gel composites and ionic liquid base gel polymer electrolyte. The detailed characterizations of these electrolytes are already described in Chapters 4 and 5. The following compositions of composite gel polymer and ionic liquid based gel polymer electrolytes are selected for the fabrication and characterization of magnesium batteries:

(a) Composite gel polymer electrolytes

[EC:PC (1:1 v/v) + 1.0M Mg(ClO₄)₂ + 20 wt.% PVdF-HFP] + 0 wt.% filler

[EC:PC (1:1 v/v) + 1.0M Mg(ClO₄)₂ + 20 wt.% PVdF-HFP] + 10 wt.% μ -MgO

[EC:PC (1:1 v/v) + 1.0M Mg(ClO₄)₂ + 20 wt.% PVdF-HFP] + 10 wt.% nano-MgO

[EC:PC (1:1 v/v) + 1.0M Mg(ClO₄)₂ + 20 wt.% PVdF-HFP] + 10 wt.% nano-SiO₂

[EC:PC (1:1 v/v) + 1.0M Mg(ClO₄)₂ + 20 wt.% PVdF-HFP] + 3 wt.% nano-SiO₂

(b) Ionic liquid based gel electrolyte

0.3M Mg(Tf)₂ in EMITf/ PVdF-HFP (4:1 ratio)

Suitable negative electrode (anode) and positive electrode (cathode) materials were prepared in order to fabricate all solid state magnesium batteries. Commercially available MnO_2 and MoO_3 were used as cathode materials. A conducting polymer, polyaniline was synthesized in the forms of bulk and nanofibres to use as a cathode materials in magnesium batteries. The Mg cells have been characterized by charge-discharge studies at room temperature ($\sim 20^\circ\text{C}$) under different constant current conditions. In addition to charge-discharge method, the electrochemical impedance of the Mg-cells has also been measured by a.c. impedance spectroscopic technique. The details are discussed in the following sections.

6.2.1 Preparation of Electrode Materials

6.2.1.1 Negative electrode (anode) preparation

Magnesium anode in the form of circular discs (area = 1.3 cm^2) were obtained by palletising the magnesium powder. These discs were polished with successive grades of emery papers to a smooth finish then washed thoroughly in acetone and dried. The mixture of graphite and magnesium has also been used as anode to fabricate Mg-cells. The graphite and magnesium powder (1:1 ratio) were thoroughly mixed and then palletised and polished.

6.2.1.2 Positive electrode (cathode) preparation

Different cathode materials were used in the present studies, viz. MnO_2 , MoO_3 and polyaniline (bulk and nanofibres).

(a) Preparation of oxide cathode materials

The work has been started with the commercially available manganese dioxide (MnO_2) and molybdenum (VI) oxide (MoO_3). These oxides were used as cathode materials by other workers for Mg-batteries [Kumar & Munichandraiah 2001; Spahr et al 1995]. Orthorhombic MoO_3 is a good intercalation host for diverse monovalent and multivalent cations [Novak et al 1999]. The intercalation properties of MoO_3 are due to its unique layered structure, as shown in Fig. 6.4 [Spahr et al 1995]. Edge and corner sharing [MoO_6] octahedral builds up double layers. These layer planes are held together by weak van der Waals attraction force. The interlayer distance has been determined to be 6.929 \AA [Kihlberg 1963]. Guest ions like Li^+ or Mg^{2+} are easily accommodated between the layers; the layers are preserved during intercalation/de-intercalation cycles. The host properties of MoO_3 admit the electrochemical intercalation of divalent magnesium cations [Spahr et al 1995].

To prepare cathode sheets, a mixture of MnO_2 or MoO_3 (75%), acetylene black (15%) as a conductive additive and PVdF-HFP (10%) of the gel polymer composition as the binder

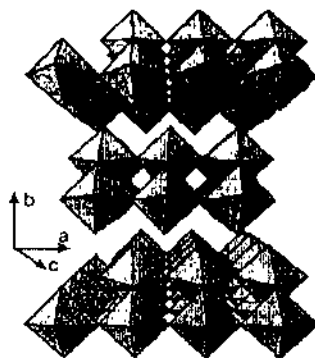


Fig. 6.4: The crystal structure of MoO_3 [Novak et al 1999].

was thoroughly ground in a mortar and spread over graphite sheet using spin coater (Apex instruments). The sheets were dried in vacuum at temperature of $\sim 90^\circ\text{C}$.

(b) Synthesis of polyaniline

Route-I (bulk polyaniline): Polyaniline has been synthesized by chemical oxidation of aniline [MacDiarmid et al 1985; Scherr et al 1991]. Aniline monomer (Aldrich) was vacuum distilled twice before use to remove impurities. These impurities, generally, create hindrance in chemical polymerization, percentage yield and physico-chemical properties of polyaniline. Pre-cooled aqueous solution of 0.5 M aniline monomer was taken in a reactor bath. Temperature of the reactor bath was maintained at $\sim 0\text{-}5^\circ\text{C}$, which favours proper polymerization of monomers. 0.1 M HCl containing $(\text{NH}_4)_2\text{S}_2\text{O}_8$ as oxidizing agent was then mixed drop wise in few hours. The pH of the solution was maintained at ~ 3.0 to avoid the formation of oligomers and other compounds. The chemical polymerization takes 24 hours to complete with proper magnetic stirring. The product was then filtered and washed repeatedly with aqueous acid solution and methanol, to remove oligomers and byproducts, until the washings were found colorless. The resultant material was vacuum dried at $\sim 60\text{-}80^\circ\text{C}$ for 12 hours to remove the water vapor and other volatile compounds. This resulting form of polyaniline is referred as conducting emeraldine salt, which is unstable and insoluble in any solvent. To make emeraldine base (stable form), emeraldine salt was mixed in 0.5 M solution of NH_4OH , stirred for 10 hours and pH was maintained at ~ 9.0 . The resulting precipitate was again filtered and washed with aqueous acid solution and methanol until the washings were found colorless. Material was vacuum dried $60\text{-}80^\circ\text{C}$ for 12 hours. Thus, conducting polymer 'polyaniline' is ready for applications.

Route-II (polyaniline nanofibres): Polyaniline nanofibres were synthesized by interfacial polymerization as reported in literature [Huang et al 2003], which is briefly described as follows. A 0.3 M sample of aniline was dissolved in chloroform (CH_2Cl_2). Ammonium

persulphate (0.075 M) was dissolved in water containing 1.0 M of HClO_4 . This aqueous solution was carefully spread over the above organic solution of monomer and kept undisturbed at $\sim 25^\circ\text{C}$ for 24 h. The solution was filtered using centrifuge, and then washed with water and acetonitrile until the filtrate was colourless. Doping and de-doping of the polymer was achieved by stirring the polymer in 1.0 M HClO_4 and 0.5 M NH_4OH , respectively, for 15 h. Then, it was filtered and vacuum dried at 40°C overnight.

The morphological structure of the polyaniline bulk and nanofibre was examined using a scanning electron microscope (Leo 440 Oxford microscopy, UK). Fig 6.5 shows the SEM pictures of polyaniline bulk and nanofibres. SEM analysis of the polyaniline prepared by this route revealed a nanofibrous structure of fibres with diameters of ~ 100 nm and lengths of ~ 450 nm. The electrical conductivity of the polyaniline nanofibres, prepared by this route, has been reported to be $\sim 0.5 \text{ S cm}^{-1}$ [Huang et al 2003].

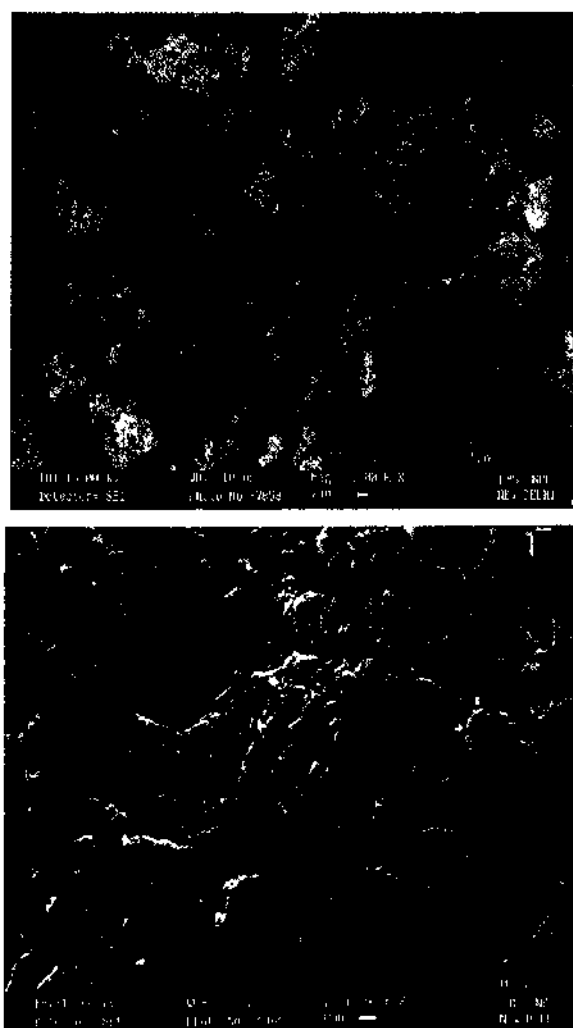


Fig. 6.5: Scanning electron micrographs of polyaniline: (a) bulk and (b) nanofibres.

To prepare the polymer cathode thick films, polyaniline bulk or nanofibres (75 wt.%) were mixed with acetylene black (15%) as a conductive additive and PVDF-HFP gel polymer composition (10%) as the binder. The resulting mixture was thoroughly ground in a mortar and spread over graphite sheet. The electrode was dried in a vacuum oven at temperature ~ 50 °C before use.

6.2.2 Fabrication and Characterization of Solid State Magnesium Batteries

Typical cells using the optimised gel composite and ionic liquid based gel polymer electrolytes have been fabricated with different anode and cathode materials. Anode| gel electrolyte |cathode cells have been assembled by sandwiching the respective electrodes and gel polymer electrolyte film in a sealed containers. The different cell configurations are listed in Table 6.2.

Table 6.2: Different cells configuration, fabricated in the present studies.

Cells	Anode	Electrolyte	Cathode
Cell-1	Mg	gel composite (10 wt.% μ MgO)	$MnO_2 + C +$ electrolyte
Cell-2	Mg	gel composite (10 wt.% SiO_2)	$MnO_2 + C +$ electrolyte
Cell-3	Mg	gel composite (10 wt.% nano MgO)	$MoO_3 + C +$ electrolyte
Cell-4	Mg	gel composite (10 wt.% μ MgO)	$MoO_3 + C +$ electrolyte
Cell-5	Mg	gel composite (10 wt.% SiO_2)	$MoO_3 + C +$ electrolyte
Cell-6	Mg	IL based gel polymer electrolyte	$MoO_3 + C +$ electrolyte
Cell-7	Mg	IL based gel polymer electrolyte	PANI+B(HCl doped) + C
Cell-8*	Mg	gel composite (10 wt.% SiO_2)	PANI (EB) + C
Cell-9*	Mg	gel composite (10 wt.% μ MgO)	PANI (EB) + C
Cell-10	Mg	gel composite (10 wt.% nano MgO)	PANI+B(HCl doped) + C
Cell-11	Mg	gel composite (10 wt.% micro MgO)	PANI+B(HCl doped) + C
Cell-12	Mg	gel composite (10 wt.% nano SiO_2)	PANI+B(HCl doped) + C
Cell-13	Mg	gel composite (10 wt.% nano SiO_2)	PANI+B(HCl doped) + C
Cell-14	Mg	gel polymer (filler free)	PANI+B(HCl doped) + C
Cell-15	Mg	gel composite (10 wt.% nano MgO)	PANI+B(HCl doped) + C
Cell-16	Mg	gel composite (10 wt.% micro MgO)	PANI+B(HCl doped) + C
Cell-17	Mg	gel composite (3 wt.% SiO_2)	PANI+B(HCl doped) + C
Cell-18	Mg	gel composite (3 wt.% SiO_2)	PANI+N ($HClO_4$ doped) +C
Cell-19	Mg	gel composite (10 wt.% nano MgO)	PANI+N ($HClO_4$ doped) +C
Cell-20	C+Mg	gel composite (with 3 wt.% SiO_2)	PANI+N ($HClO_4$ doped) +C

* Primary cells

The typical experimental set up for the charge-discharge characterization of the batteries along with the cells is shown in Fig. 6.6. The open circuit voltage (OCV) has been measured for ~ 50 -100 h to ensure proper electrode-electrolyte contacts and to check the voltage stability with time. The open-circuit voltages of Mg-cells have been found to be in the range of 1.6-1.95 V. Fig. 6.7 shows the 'OCV vs. time' plots of some typical Mg-cells.



Fig. 6.6: The typical experimental set up along with the Mg-cells.

The OCV values of the cells: Mg/gel electrolyte/oxide cathodes are stable with time whereas the Mg/gel electrolyte/ polyaniline (PANI) cells decreases initially with time and then become constant. One of the most important limitations of polyaniline, concerning their application as cathode electrode in rechargeable batteries, is that they are self-discharged with a relatively high rate which causes the decrease in OCV of the batteries. Several workers have reported the reduction in OCV of Zn-PANI batteries and suggested various explanations [Mengoli et al 1987; Trinidad et al 1991; Mu et al 1993]. Trinidad et al. [1991] proposed that the observed OCV reduction of the battery may be attributed to some unknown redox reactions and/or to a non-reversible diffusion effect of counter anions to electrolyte.

The interfacial behaviour of the cells was investigated by a.c. impedance measurements. Fig. 6.8 shows complex impedance plots of some typical Mg cells at room temperature (~ 20 °C). The impedance response showed a low interfacial resistance (~ 30 -40 Ω) at high frequency region, which is comparable to the value reported for Li-PANI cell [Sivakkumar et al 2007].

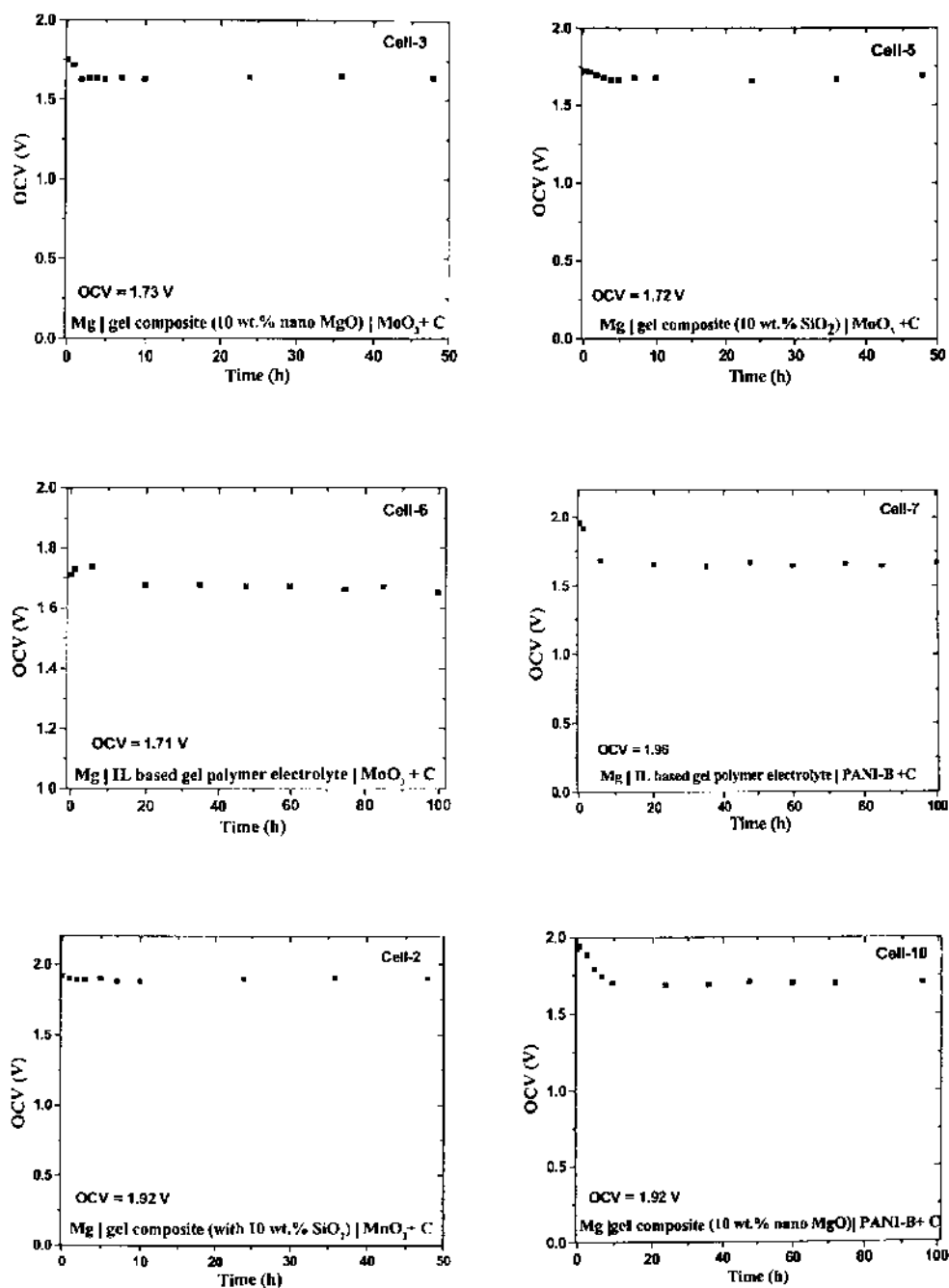


Fig. 6.7: 'OCV vs. time' plots for some typical Mg cells.

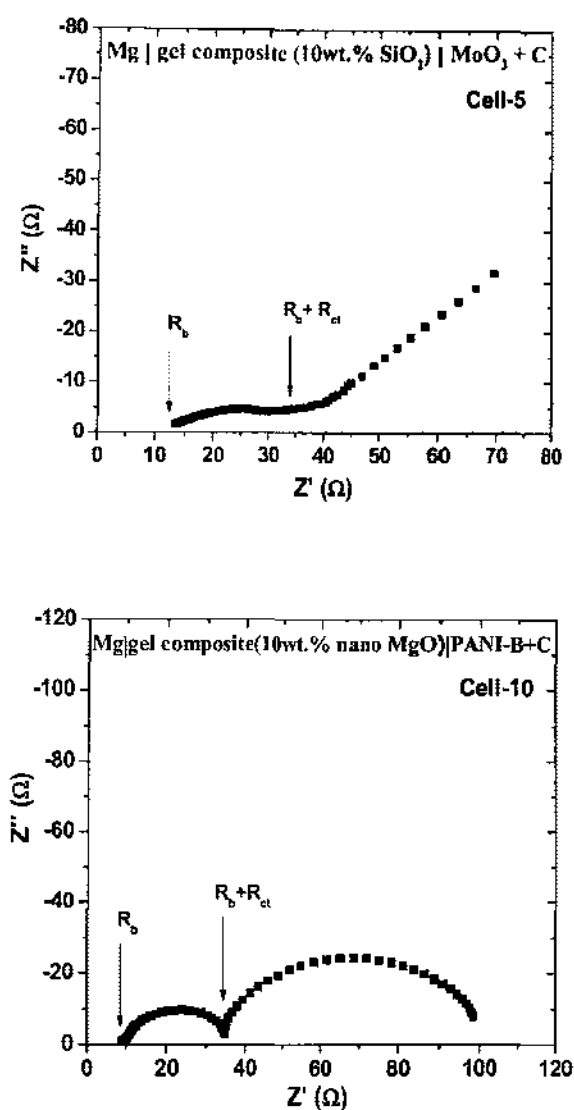


Fig. 6.8: Complex impedance plots of some typical Mg cells at room temperature (~ 20 °C).

The galvanostatic charge-discharge characteristic studies have been carried out for all the cells listed in Table 6.2. As mentioned earlier in Chapter 2, these studies have been carried out using Arbin instrument (model: BT 2000, USA) under different constant current conditions. The charge-discharge behaviour of these different cell configurations are shown in Fig. 6.9, 6.10 & 6.11. The different cell parameters viz. discharge capacity, discharge energy and specific power have been calculated for the first discharge curve and listed in Table 6.3. On the basis of these studies the following important features have been drawn:

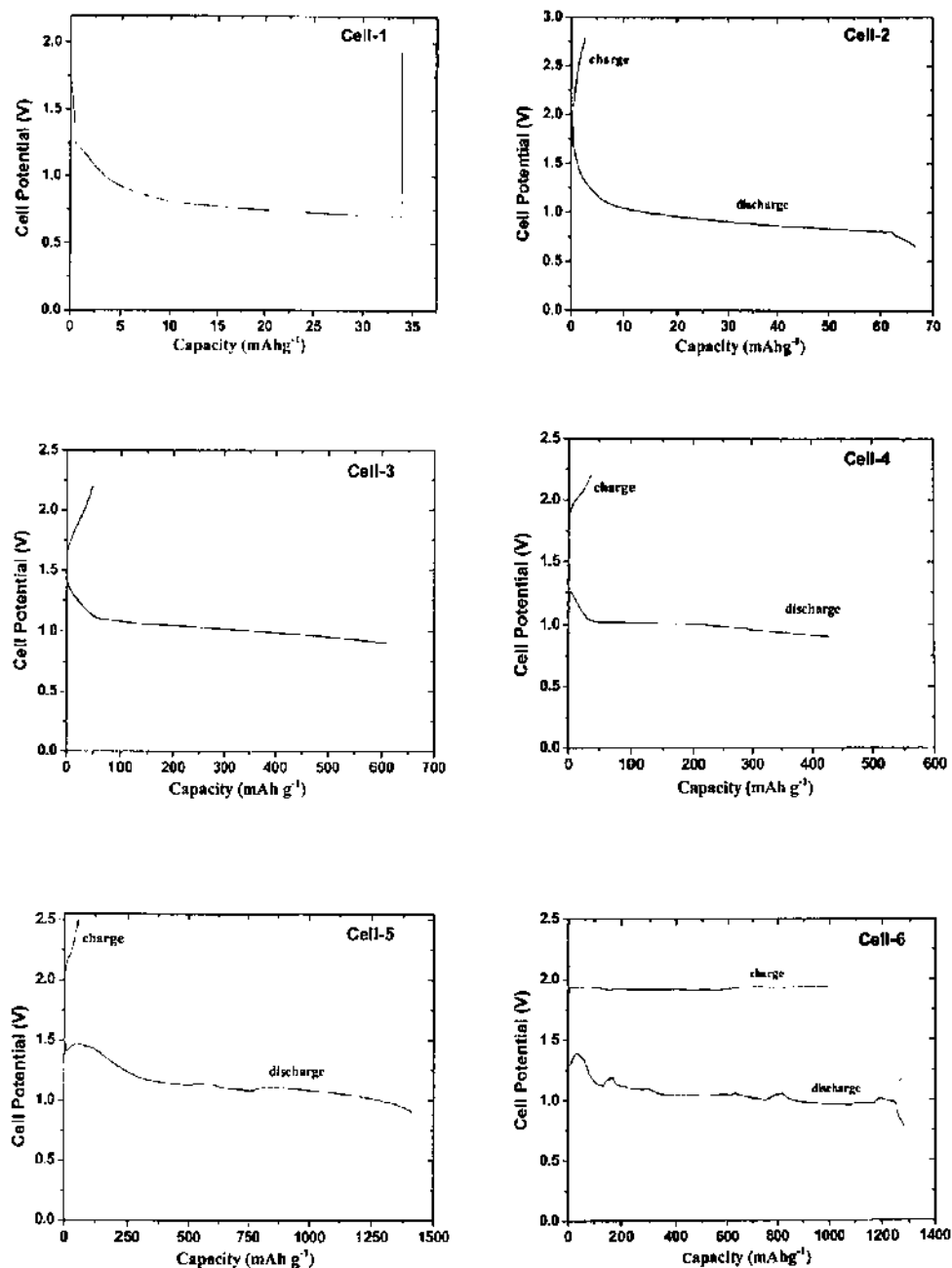


Fig. 6.9: Discharge and charge profiles of different Mg cells at room temperature ($\sim 20^\circ\text{C}$). Cell number in the figure represents the corresponding cell configuration listed in Table 6.2.

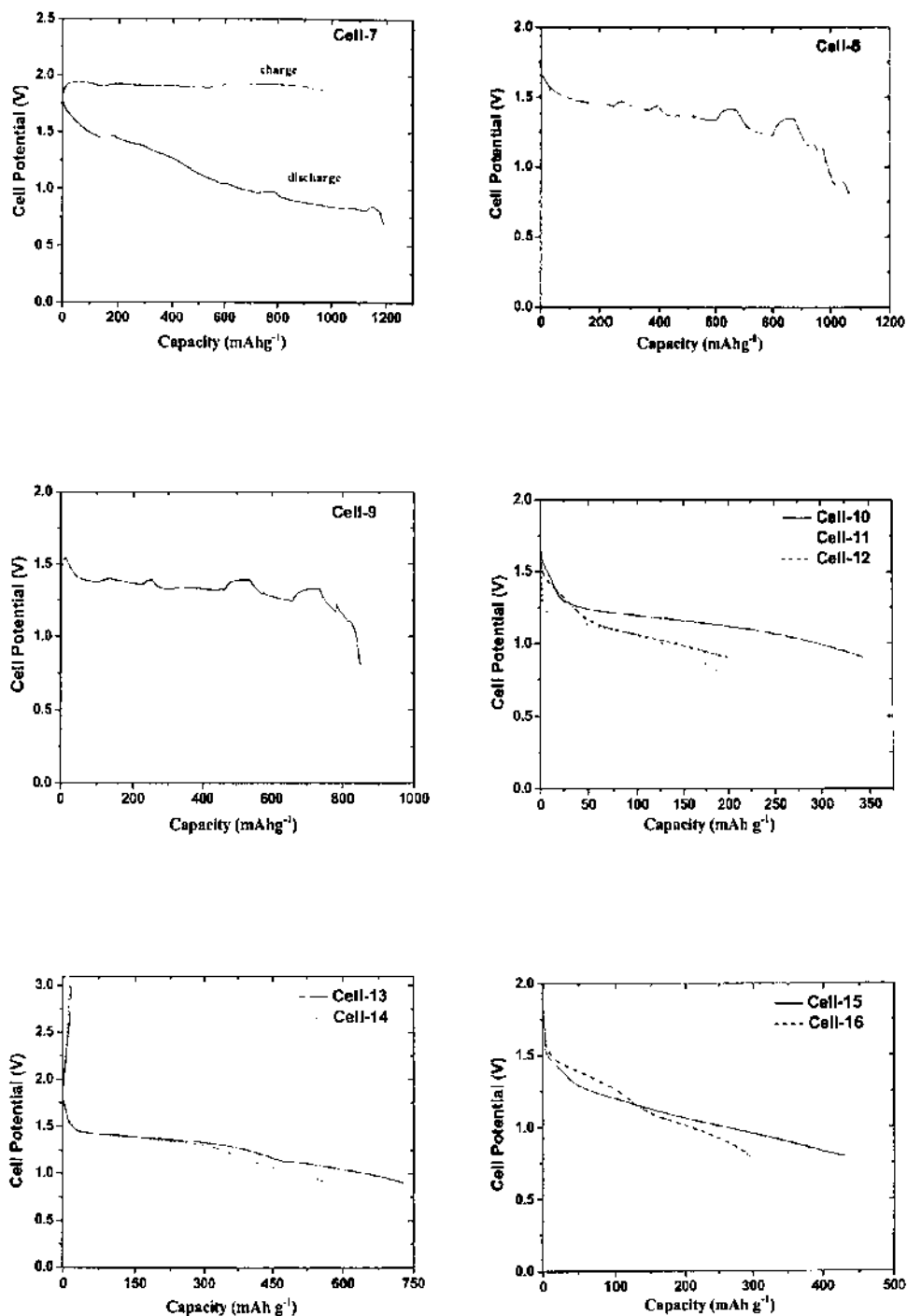


Fig. 6.10: Discharge and charge profiles of different Mg cells at room temperature (~ 20 °C). Cell number in the figure represents the corresponding cell configuration listed in Table 6.2.

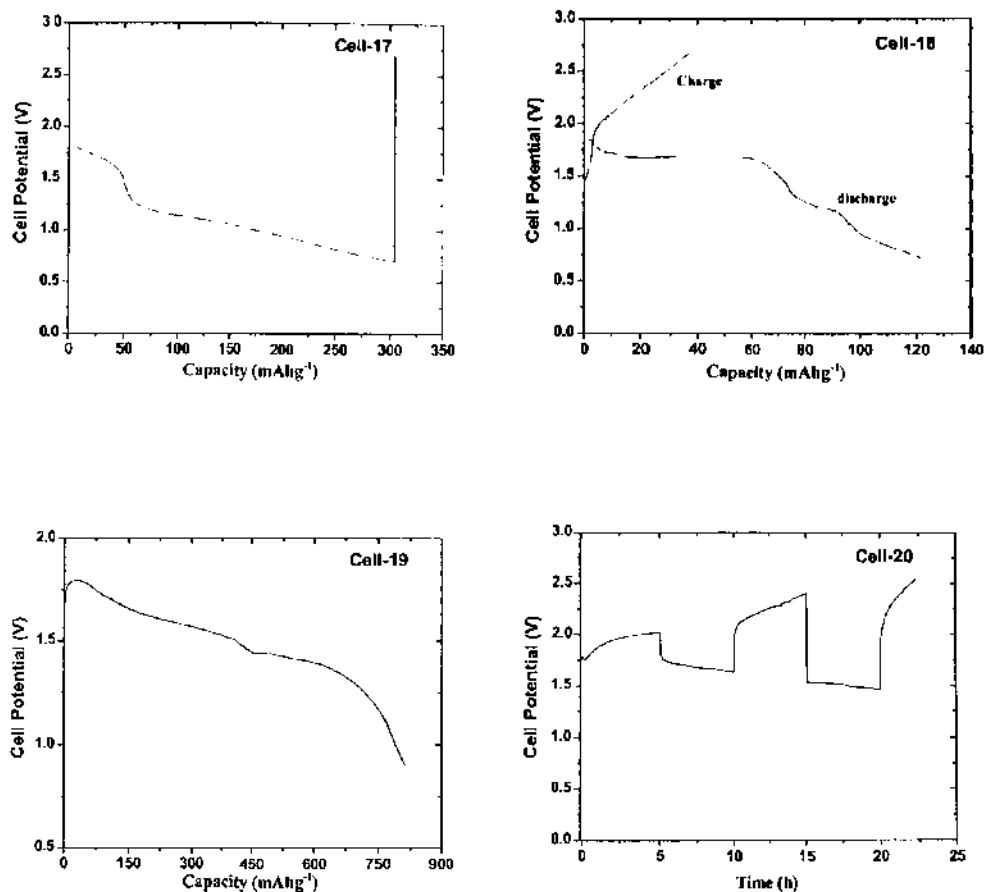


Fig. 6.11: Discharge and charge profiles of different Mg cells at room temperature ($\sim 20^\circ\text{C}$). Cell number in the figure represents the corresponding cell configuration listed in Table 6.2.

- (1) For Mg/MnO₂ cells (Fig. 6.9, Cell-1 and Cell-2) a potential plateau has been observed at $\sim 0.8\text{--}0.9\text{ V}$ during their discharge. The first discharge capacity is about $35\text{--}65\text{ mAh g}^{-1}$ of MnO₂. However, the cells have very low capacity for charging. The cell overvoltage was rather high despite the low current density ($100\ \mu\text{A cm}^{-2}$). This may be due to the electrochemical irreversibility of metallic magnesium.
- (2) For Mg/MoO₃ cells (Fig. 6.9, Cells- 3, 4 and 5), a potential plateau was observed at $\sim 1\text{ V}$ during the discharge. The first discharge capacity is high and about $600\text{--}1350\text{ mAh g}^{-1}$ of MoO₃. However, the cells have poor rechargeability, possibly due to the passivating surface film formation on Mg anode.
- (3) The ionic liquid gel polymer electrolyte based cells with MoO₃ and polyaniline (bulk, HCl doped) (Fig. 6.9, Cell-6 and Fig. 6.10, Cell-7) show very high discharge capacity of

~ 1200 mAh g⁻¹. The cells show good capacity of charging initially only for 2-3 cycles, thereafter they perform poor rechargeability.

Table 6.3: The different cell parameters of Mg-batteries.

Cells	OCV (V)	Working voltage (V)	Current Density ($\mu\text{A cm}^{-2}$)	Discharge capacity (mAh g ⁻¹)	Discharge Energy (Wh g ⁻¹)	Power Density (mW g ⁻¹)
Cell-1	1.85	0.8	100	35	0.0275	17.5
Cell-2	1.92	0.9	100	65	0.0625	25
Cell-3	1.73	1.0	100	600	0.625	25
Cell-4	1.72	1.0	100	430	0.425	20
Cell-5	1.61	1.0	200	1350	1.6	46
Cell-6	1.71	1.0	75	1250	1.32	14.8
Cell-7	1.96	1.0	75	1200	1.33	11.8
Cell-8	1.81	1.3	100	1050	1.42	16
Cell-9	1.70	1.35	100	850	1.12	22
Cell-10	1.71	1.2	500	300	0.393	137
Cell-11	1.72	1.1	500	200	0.198	137.5
Cell-12	1.81	1.1	500	200	0.22	140
Cell-13	1.88	1.35	200	450	0.902	56
Cell-14	1.89	1.35	200	350	0.70	54
Cell-15	1.81	1.0	1000	350	0.450	250
Cell-16	1.71	1.0	1000	250	0.337	250
Cell-17	1.82	1.1	100	200	0.282	22.5
Cell-18	1.91	1.6	100	100	0.086	30
Cell-19	1.95	1.4	200	650	1.17	211
Cell-20	1.76	-	-	-	-	-

- (4) Two primary Mg/PANI (EB = emeraldine base, stable form, undoped) cells (Fig. 6.10, Cells-8 and 9) were fabricated and characterized, which show intermittent type discharge behaviour. In this behaviour, the cell has the opportunity to recover from polarization effects during lengthy discharges. The voltage recovery of cell is dependent on current drain (generally greater after the higher current drains) as well as on particular battery system, discharge temperature and end voltage etc. [Linden 2002].
- (5) Some Mg/PANI-B (bulk, HCl doped) cells (Fig. 6.10, Cells 10-16) have been fabricated and discharged through different constant current conditions (200, 500 and 1000 $\mu\text{A cm}^{-2}$). For low current drain (200 $\mu\text{A cm}^{-2}$), the potential plateau has been observed at

- ~ 1.35 V during the discharge. All the cells show good discharge capacity (~ 200-450 mAh g⁻¹) for the first discharge curve, but poor rechargeability.
- (6) To compare the performance of two forms of polyaniline (bulk and nanofibres polyaniline) as cathode materials, Mg cells were fabricated with a composite gel polymer electrolyte (with 3 wt.% SiO₂) (Fig. 6.11 Cell-17, with PANI-B and Cell-18, with PANI-N). Both the cells show two-step discharge profiles, which indicate a change in the reaction mechanism and potential of the active material. Mg/PANI-B cell (Fig. 6.11 Cell-17) has very poor capacity for recharging while; Mg/PANI-N cell (Fig. 6.11 Cell-18) has recharge for first cycle upto 40 mAh g⁻¹. For subsequent cycles the cell shows low charge capacity, probably due to high impedance at the interface between Mg metal and the gel polymer electrolyte. Nevertheless, nanofibre polyaniline has proved its potential as a good cathode material for rechargeable Mg-batteries.
- (7) As discussed above, Mg cells with various cathode materials show poor rechargeability, most possibly due to the passivating surface film formation on Mg anode, which increase the charge transfer resistance at Mg/gel electrolyte interface. Therefore, a mixture of magnesium and graphite powder has been used as an anode material. A C+Mg/PANI-N cell have been fabricated and characterized. For this cell (Fig. 6.11, Cell-20) a potential plateau has been observed at ~1.76 V during the discharge. The cell shows good charge capacity only for 3-4 cycles. This result provides an alternative anode material for Mg²⁺-ion battery, however, further extensive works are required.

6.3 Conclusions

Solid State proton and magnesium batteries using respectively the optimized proton and magnesium ion conducting polymer/gel electrolytes have been fabricated and characterized. All-solid-state polymeric proton batteries have been fabricated using proton conducting nanocomposite polymer electrolytes PEO:NH₄HSO₄ (92:8 w/w) +3 wt.%SiO₂ (solution cast) and PEO:NH₄HSO₄ (80:20 w/w) +15 wt.%SiO₂ (hot-pressed). The mixture of Zn + ZnSO₄.7H₂O was used as anode and mixtures of MnO₂+C (6:4 ratio) + polymer electrolyte and layered oxides PbO₂+V₂O₅+C (7:2:1 ratio) + polymer electrolyte were used as cathode materials. The batteries were discharged through two load resistances 1 MΩ and 100 KΩ. It has been observed that the cell potentials remained stable, after the usual initial potential drop due to polarization effect, for long time during low current drain (~ 1μA). However, it has been discharged more quickly during higher current drain or with low load resistance. Thus, the cells have been found to be suitable for low current density applications.

The magnesium rechargeable batteries have been fabricated using optimized composite gel polymer electrolytes EC:PC+Mg(ClO₄)₂+PVdF-HFP dispersed with different fillers (micro and nanosized MgO, and nanosized SiO₂) and ionic liquid based gel polymer electrolyte Mg(Tf)₂ /EMITf/ PVdF-HFP. Pressed pellets of Mg powder or Mg-graphite mixture were used as anode, whereas MnO₂, MoO₃ and polyaniline (bulk and nanofibres) were used as cathode materials. On the basis of the galvanostatic charge-discharge studies, the following conclusions have been drawn:

- (i) The studies suggest the suitability of composite gel polymer electrolytes and ionic liquid based gel polymer electrolyte in the development of magnesium rechargeable batteries.
- (ii) The best capacity and discharge energy density have been obtained for the cells with MoO₃ based cathode material. However, the better rechargeability has been observed for the cells with the nano-fibrous polyaniline cathodes.
- (iii) The poor rechargeability of Mg cells is probably due to the passivation of Mg electrode at Mg/gel electrolyte interface.
- (iv) Carbon mixed with Mg powder anode material can be used to develop Mg-ion rechargeable batteries analogous to Li-ion battery system.
- (v) These studies show the prospect of rechargeable magnesium batteries with solid-like gel polymer electrolytes, however, further extensive investigations are required to improve the performance of the Mg-based rechargeable batteries.